Available online at www.eccomasproceedia.org
Eccomas Proceedia COMPDYN (2017) 3763-3770

ECCOMAS
Proceedia

COMPDYN 2017
6th ECCOMAS Thematic Conference on
Computational Methods in Structural Dynamics and Earthquake Engineering
M. Papadrakakis, M. Fragiadakis (eds.)
Rhodes Island, Greece, 15–17 June, 2017

FLUTTER ANALYSIS OF COMPOSITE LAMINATES WITH CURVILINEAR FIBRES

Hamed Akhavan and Pedro Ribeiro

DEMec/INEGI, Faculdade de Engenharia, Universidade do Porto
Rua Dr. Roberto Frias, s/n 4200-465, Porto, PORTUGAL
e-mail: {hamed,pmleal}@fe.up.pt

Keywords: Flutter, Composite Plate, Piston Theory, Curvilinear Fibres, Variable Stiffness.

Abstract. *In this investigation, the authors intend to study the dynamic instability (flutter) of variable stiffness composite laminates (VSCLs) in the presence of supersonic flow. In the type of VSCL considered here, plies have curvilinear fibres and, consequently, the stiffness is variable in a macroscopic view. The plates considered are rectangular. In each ply, a reference fibre path, represented by a function of horizontal coordinate x, is defined. The reference fibre path orientation changes linearly from* T_0 *at the centre to* T_1 *at both vertical edges of the ply; the other fibre paths are defined shifting the reference path in direction y. The displacement and rotations are defined using a Third-order Shear Deformation Theory, and then they are discretised by a p-version finite element model that applies to VSCL plates. Piston theory is employed to model the aerodynamic force of the upstream flow in direction x. Flutter airspeeds are investigated for VSCL plates with different fibre angles. Changes of flutter speed are evaluated in two different regimes of steady and unsteady flow.*

doi: 10.7712/120117.5682.17469

1 INTRODUCTION

The traditional fibrous composite panels consist of fibres placed with various angles (orientations) in the matrix of each ply. From a macroscopic point of view, the in-plane and the bending stiffness of the panel do not change from one point to the other. In complex structures where fibrous composite panels are used, load and stress distributions in different regions of the panel are not uniform. To reinforce the regions of high stress, two methods were before used: increasing the thicknesses or mounting stiffeners. These two techniques alter the final shape of the design by occupying more space and increasing the weight. The variable stiffness concept using curvilinear fibres [1, 2, 3] can propose a panel with different, and under-controlled stiffness. This concept suggests to rotate fibre orientation in a region with high stress.

The promising capabilities of composite laminates with curvilinear fibre paths based on their linear vibration behaviour [4, 5, 6], static behaviour [7, 8], stress re-distribution and (post)buckling [9, 10], and non-linear vibrations [11, 12] are already demonstrated. These references reported higher natural frequencies, less static deflection, different stress re-distribution and different dynamics of composite plates consisting of curvilinear fibre paths. Also, higher buckling loads and failure onsets are predicted using this type of fibre paths. As far as aeroelasticity is concerned, there are not enough studies explaining the flutter modes and behaviour of such plates. In some investigations [13, 14], flutter of wings have been controlled by adding curvilinear stiffeners. About the composite laminates with curvilinear fibres, [15] used a genetic algorithm to find the impact of various tailoring choices including curvilinear fibre orientation and stacking sequence upon the flutter.

As it is understood, the use of curvilinear fibres to control flutter has received relatively little attention in the literature. In this paper, supersonic flutter of a variable stiffness composite laminate (VSCL) - composite laminates with curvilinear fibres - is investigated. The target is to search for improvements in flutter of such plates against constant stiffness composite plates (CSCL) where straight fibres are used. A third-order shear deformation theory is used to model the displacements of the plate. Displacements and rotation of a general point in the mid-plane are discretised using a *p*-version finite element [16, 17]. The plate is in the presence of a supersonic flow. To model the aerodynamic force of the upstream flow, Piston theory [18] is employed. The equations of motion, in the form of an eigenvalue problem, are solved to find the flutter speed. The eigenvalues of such system are complex.

Flutter speeds of VSCLs with different boundary conditions including clamped and free boundaries against various tow orientations are evaluated. VSCLs with other boundaries are under investigation. The aim of this study is to investigate how does the flutter speed vary in VSCLs with diverse fibre angles at the centre and edges of the plates.

2 EIGENVALUE PROBLEM OF VSCL PLATES WITH PISTON THEORY

Figure 1a displays the schematic of the plate. The rectangular VSCL has length a, width b, and thickness h, where a right-handed three-dimensional Cartesian coordinate system x, y, z is adopted, with the origin of the coordinate system located in the geometric centre of the undeformed plate. The laminate is symmetric about its middle surface, consisting of 12 composite layers with curvilinear fibre paths. The reference fibre path is defined in the form of

$$\theta\left(x\right) = 2\left(T_1 - T_0\right)\frac{|x|}{a} + T_0 \tag{1}$$

where T_0 and T_1 are the fibre path angles in the centre and vertical edges of the ply (Figure 1b). The angle of the reference fibre path, θ, is a linear function of the *x*-coordinate and, in order to define the other fibre paths, this reference fibre path is shifted in y-direction [2].

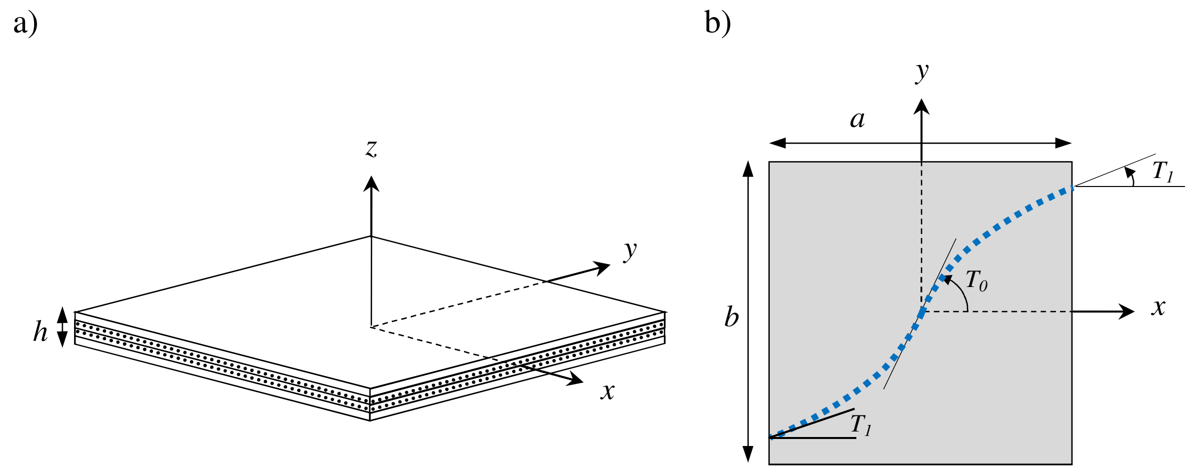

Figure 1: a) geometry of the laminate and b) curvilinear fibre path.

Fig 1. A symmetric laminate including a reference curvilinear fibre path in a flat ply.

A displacement field based on third-order shear deformation theory [19, 20] is used as follows

$$u(x,y,z,t) = u^0(x,y,t) + z\phi_x(x,y,t) - cz^3\left(\phi_x(x,y,t) + \frac{\partial w^0(x,y,t)}{\partial x}\right) \tag{2}$$

$$v(x,y,z,t) = v^0(x,y,t) + z\phi_y(x,y,t) - cz^3\left(\phi_y(x,y,t) + \frac{\partial w^0(x,y,t)}{\partial y}\right)$$

$$w(x,y,z,t) = w^0(x,y,t)$$

Here, u, v, and w are the displacement components in the x, y, and z directions; u^0, v^0, and w^0 are their values at the mid-plane and ϕ_x and ϕ_y are the independent rotations of the normal to the middle surface about the y and x axis, respectively. t is time and $c = 4/3h^2$. Mid-plane displacements and rotations are discretised using a *p*-version finite element as

$$\begin{Bmatrix} u^0(x,y,t) \\ v^0(x,y,t) \\ w^0(x,y,t) \\ \phi_x(x,y,t) \\ \phi_y(x,y,t) \end{Bmatrix} = \begin{bmatrix} \mathbf{N^u}(x,y)^T & \mathbf{0} & \mathbf{0} & \mathbf{0} & \mathbf{0} \\ \mathbf{0} & \mathbf{N^u}(x,y)^T & \mathbf{0} & \mathbf{0} & \mathbf{0} \\ \mathbf{0} & \mathbf{0} & \mathbf{N^w}(x,y)^T & \mathbf{0} & \mathbf{0} \\ \mathbf{0} & \mathbf{0} & \mathbf{0} & \mathbf{N}^{\phi_\mathbf{x}}(x,y)^T & \mathbf{0} \\ \mathbf{0} & \mathbf{0} & \mathbf{0} & \mathbf{0} & \mathbf{N}^{\phi_\mathbf{y}}(x,y)^T \end{bmatrix} \begin{Bmatrix} \mathbf{q_u}(t) \\ \mathbf{q_v}(t) \\ \mathbf{q_w}(t) \\ \mathbf{q}_{\phi_\mathbf{x}}(t) \\ \mathbf{q}_{\phi_\mathbf{y}}(t) \end{Bmatrix} \tag{3}$$

where $\mathbf{N^i}(x,y)$ are vector of shape functions and $\mathbf{q_i}(t)$ are generalised displacement vectors ($\mathbf{i}=$ $\mathbf{u}$, $\mathbf{v}$, $\mathbf{w}$, $\boldsymbol{\phi}_\mathbf{x}$, and $\boldsymbol{\phi}_\mathbf{y}$) [16, 17].

The stress-strain relation (in material coordinates i.e. the fibre direction and perpendicular to the fibre direction) of an orthotropic lamina is valid in each arbitrary point of the ply made of curvilinear fibres. Because of the rotation of the fibre path $\theta(x)$, the stresses and strains can be rotated from their material coordinates to the global coordinates (x and y) using transformation matrix [1]. The strain displacement relations in the linear regime are considered here.

The flutter pressure - pressure on upper surface of the plate while the lower surface has static pressure - due to a supersonic flow (highly unsteady) is introduced by Piston theory [18]

$$\Delta P\left(x,y,t\right) = -\frac{\rho_\infty {U_\infty}^2}{M}\left(\frac{1}{U_\infty}w_{,t} + w_{,x}\right) \tag{4}$$

in which ρ_∞ is upstream far-field density, U_∞ velocity of the flow, and M local Mach number. By removing the derivative in terms of time $w_{,t}$, the analysis is is in the steady regime. Substituting terms of shape functions and generalized coordinates, Equation 3, in flutter pressure of Equation 4 and subsequently using the principle of virtual work gives the equations of motion as

$$\begin{bmatrix} \mathbf{M}^{11} & \mathbf{0} & \mathbf{0} & \mathbf{0} & \mathbf{0} \\ & \mathbf{M}^{22} & \mathbf{0} & \mathbf{0} & \mathbf{0} \\ & & \mathbf{M}^{33} & \mathbf{M}^{34} & \mathbf{M}^{35} \\ & & & \mathbf{M}^{44} & \mathbf{0} \\ sym & & & & \mathbf{M}^{55} \end{bmatrix} \begin{Bmatrix} \ddot{\mathbf{q}}_\mathbf{u} \\ \ddot{\mathbf{q}}_\mathbf{v} \\ \ddot{\mathbf{q}}_\mathbf{w} \\ \ddot{\mathbf{q}}_{\phi_\mathbf{x}} \\ \ddot{\mathbf{q}}_{\phi_\mathbf{y}} \end{Bmatrix} + \begin{bmatrix} \mathbf{K}_\mathbf{L}^{11} & \mathbf{K}_\mathbf{L}^{12} & \mathbf{K}_\mathbf{L}^{13} & \mathbf{0} & \mathbf{0} \\ & \mathbf{K}_\mathbf{L}^{22} & \mathbf{K}_\mathbf{L}^{23} & \mathbf{0} & \mathbf{0} \\ & & \mathbf{K}_\mathbf{L}^{33} & \mathbf{K}_\mathbf{L}^{34} & \mathbf{K}_\mathbf{L}^{35} \\ & & & \mathbf{K}_\mathbf{L}^{44} & \mathbf{K}_\mathbf{L}^{45} \\ sym & & & & \mathbf{K}_\mathbf{L}^{55} \end{bmatrix} \begin{Bmatrix} \mathbf{q}_\mathbf{u} \\ \mathbf{q}_\mathbf{v} \\ \mathbf{q}_\mathbf{w} \\ \mathbf{q}_{\phi_\mathbf{x}} \\ \mathbf{q}_{\phi_\mathbf{y}} \end{Bmatrix} \tag{5}$$

$$+ \begin{bmatrix} \mathbf{0} & \mathbf{0} & \mathbf{0} & \mathbf{0} & \mathbf{0} \\ & \mathbf{0} & \mathbf{0} & \mathbf{0} & \mathbf{0} \\ & & \mathbf{F}^{33}_{unsteady} & \mathbf{0} & \mathbf{0} \\ & & & \mathbf{0} & \mathbf{0} \\ sym & & & & \mathbf{0} \end{bmatrix} \begin{Bmatrix} \dot{\mathbf{q}}_\mathbf{u} \\ \dot{\mathbf{q}}_\mathbf{v} \\ \dot{\mathbf{q}}_\mathbf{w} \\ \dot{\mathbf{q}}_{\phi_\mathbf{x}} \\ \dot{\mathbf{q}}_{\phi_\mathbf{y}} \end{Bmatrix} + \begin{bmatrix} \mathbf{0} & \mathbf{0} & \mathbf{0} & \mathbf{0} & \mathbf{0} \\ & \mathbf{0} & \mathbf{0} & \mathbf{0} & \mathbf{0} \\ & & \mathbf{F}^{33}_{steady} & \mathbf{0} & \mathbf{0} \\ & & & \mathbf{0} & \mathbf{0} \\ sym & & & & \mathbf{0} \end{bmatrix} \begin{Bmatrix} \mathbf{q}_\mathbf{u} \\ \mathbf{q}_\mathbf{v} \\ \mathbf{q}_\mathbf{w} \\ \mathbf{q}_{\phi_\mathbf{x}} \\ \mathbf{q}_{\phi_\mathbf{y}} \end{Bmatrix} = \mathbf{0}$$

In simplified notation, the equations of motion including viscous damping may be written in the form of $\mathbf{M}\ddot{\mathbf{q}}\left(t\right) + \left(\mathbf{F}_{unsteady} + \alpha\mathbf{M} + \beta\mathbf{K}\right)\dot{\mathbf{q}}\left(t\right) + \left(\mathbf{K_L} + \mathbf{F}_{steady}\right)\mathbf{q}\left(t\right) = \mathbf{0}$. Using $\dot{\mathbf{q}}\left(t\right) = \mathbf{y}\left(t\right)$, the second-order differential equations of motion can be transformed to first-order differential equations of motion as follows

$$\begin{bmatrix} \mathbf{M} & \mathbf{0} \\ \mathbf{0} & -\mathbf{M} \end{bmatrix} \begin{Bmatrix} \dot{\mathbf{y}}\left(t\right) \\ \dot{\mathbf{q}}\left(t\right) \end{Bmatrix} + \begin{bmatrix} \mathbf{F}_{unsteady} + \alpha\mathbf{M} + \beta\mathbf{K} & \mathbf{K_L} + \mathbf{F}_{steady} \\ \mathbf{M} & \mathbf{0} \end{bmatrix} \begin{Bmatrix} \mathbf{y}\left(t\right) \\ \mathbf{q}\left(t\right) \end{Bmatrix} = \begin{Bmatrix} \mathbf{0} \\ \mathbf{0} \end{Bmatrix} \tag{6}$$

By taking $\mathbf{q}\left(t\right) = \mathbf{q_0}^{i\omega t}$, the eigenvalue problem below is achieved,

$$i\omega \begin{bmatrix} -\mathbf{M} & \mathbf{0} \\ \mathbf{0} & \mathbf{M} \end{bmatrix} \begin{Bmatrix} \mathbf{y}\left(t\right) \\ \mathbf{q}\left(t\right) \end{Bmatrix} = \begin{bmatrix} \mathbf{F}_{unsteady} + \alpha\mathbf{M} + \beta\mathbf{K} & \mathbf{K_L} + \mathbf{F}_{steady} \\ \mathbf{M} & \mathbf{0} \end{bmatrix} \begin{Bmatrix} \mathbf{y}\left(t\right) \\ \mathbf{q}\left(t\right) \end{Bmatrix} \tag{7}$$

Here, $\mathbf{F}_{unsteady}$ represents the aerodynamic damping. Solving this eigenvalue problem results in flutter speed in the unsteady regime of flow. Neglecting the term $\mathbf{F}_{unsteady}$ gives the steady results for flutter speed. ω will be found as conjugate pairs whose real parts represent frequency and imaginary parts damping. Flutter happens if the imaginary part of at least one ω is less than zero.

3 FLUTTER OF COMPOSITE LAMINATES WITH CURVINEAR FIBRES

12-layer laminates with fibre configurations $[\langle 45° + \varphi_0, 45° + \varphi_1 \rangle, \langle -45° - \varphi_0, -45° - \varphi_1 \rangle,$ $\langle 0° + \varphi_0, 0° + \varphi_1 \rangle, \langle 0° - \varphi_0, 0° - \varphi_1 \rangle, \langle 90° + \varphi_0, 90° + \varphi_1 \rangle, \langle -90° - \varphi_0, -90° - \varphi_1 \rangle]_{sym}$ are analysed. The fibre orientations are introduced in this way: in the first layer, $T_0 = 45° + \varphi_0$ and $T_1 = 45° + \varphi_1$; in the second layer, $T_0 = -45° - \varphi_0$ and $T_1 = -45° - \varphi_1$; and so forth. Mechanical properties of the VSCL are as follows: major and minor Youngs moduli, $E_1 = 126.3$ GPa and $E_2 = 8.765$ GPa, shear moduli $G_{12} = G_{13} = 4.92$ GPa and $G_{23} = 3.35$ GPa, Poisson's ratio $\nu_{12} = 0.334$ and density $\rho = 1557$ kg/m^3. The length and width of the plate are equal to 0.5 m. The total thickness is 0.006 m and all the layers have equal thickness. It should be mentioned that when φ_0 and φ_1 angles are not equal, these fibre configurations represent VSCLs. When φ_0 and φ_1 angles are equal (e.g. 0°), the configuration represents a CSCL. For the VSCL plates analysed in the following figures, flutter speeds with changing φ_0 - shown with red star in the figures - and with changing φ_1 - shown with black diamond in the figures - are calculated in the range of fibre angle from 0° to 45°. If φ_0 is changing then $\varphi_1 = 0°$ and vice versa. The analysis is performed for VSCL with different clamped and free boundary conditions. In this study, seven one-dimensional shape functions, equal to 245 DOF, is used in the *p*-version finite element. The coefficients of viscous damping α and β are extracted from experiments [21] and are equal to 8.2×10^{-5} and -0.505, respectively.

3.1 All edges clamped

Figure 2 displays the flutter speed (shown in the vertical axis) of the clamped VSCL plates in three various situations: steady regime without viscous damping, unsteady regime without viscous damping and unsteady regime with viscous damping. It shows that performing the analysis in unsteady regime of flow - taking into consideration $w_{,t}$ in Equation 4 - increases the flutter speed. Although adding the viscous damping reduces the flutter speed in CSCL (i.e. $\varphi_0 = \varphi_1 = 0°$), this effect changes slightly in VSCLs. In all three cases, increasing φ_0 ($\varphi_1 = 0°$) or φ_1 ($\varphi_0 = 0°$) reduces the flutter speed. From this point of view and in the range of investigated VSCLs, using the curvilinear fibres has no advantage.

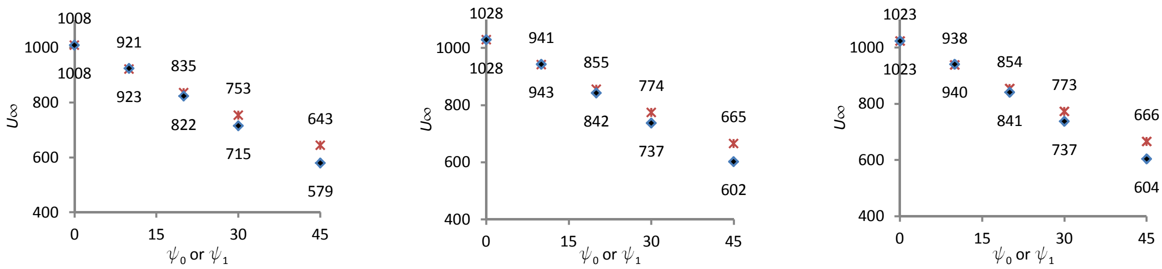

a) b) c)

Figure 2: Flutter speed of the clamped plate in a) steady regime without viscous damping, b) unsteady regime without viscous damping and c) unsteady regime with viscous damping.

3.2 All edges free

In order to include aerodynamic and structural damping into account, in free boundary condition, only flutter speeds in the unsteady regime of flow and in the presence of viscous damping are displayed. In the free plates, given in Figure 3, flutter speed always decreases with the increase of fibre angle at the centre of the plate φ_0. But, increasing φ_1 has a different effect: it first reduces the flutter speed and then leads higher flutter speeds. In the range of investigated plates, the best design in terms of flutter speed, is the CSCL with 653 m/s. The fact that increasing the fibre angle at the edges of the plate improves the flutter speed needs more investigation. Understanding different effects of fibre angles at the centre and the edges on flutter concept can help the researchers to evaluate VSCLs with other types of boundary condition or fibre angle ranges to exploit their potentials better.

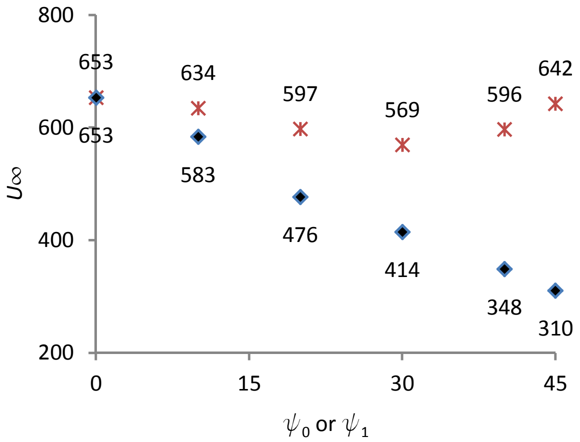

Figure 3: Flutter speed of the free plate in the unsteady regime with viscous damping.

4 CONCLUSIONS

A VSCL plate with curvilinear fibres was introduced where the fibre angle changes linearly from the centre of the ply to the edges. The flutter speed of such plate subjected to a supersonic upstream was evaluated in the steady and in the unsteady regimes of flow. A structural viscous damping proportional to the mass and the stiffness matrix was applied. Piston theory was used to model the aerodynamic pressure of the flow. The analysis was carried out for different boundary conditions including clamped and free plates. It was shown that in clamped and free VSCL plates, the flutter speed always decreases with the increase of the fibre angles at the centre of the plate. In other words, the clamped and free composite laminates with curvilinear fibres at the centre did not show any advantage in comparison to laminates with straight fibres. As far as free plate is concerned, only with increasing the fibre angle at the edges ($\varphi_1 > 30°$) the flutter speed increases. The potential possibilities to increase the flutter speed of VSCL plates with the concept of curvilinear fibres requires to be uncovered with consideration of different boundary conditions and various range of fibre angle orientations.

ACKNOWLEDGEMENTS

The authors gratefully acknowledge the funding of Project NORTE-01-0145-FEDER-000022 - SciTech - Science and Technology for Competitive and Sustainable Industries, cofinanced by Programa Operacional Regional do Norte (NORTE2020), through Fundo Europeu de Desenvolvimento Regional (FEDER).

REFERENCES

[1] H. Akhavan, *Non-linear vibrations of tow placed variable stiffness composite laminates*. PhD Thesis, University of Porto, Portugal, 2015.

[2] C. Waldhart, *Analysis of tow-placed, variable-stiffness laminates*. Master Thesis, Virginia Polytechnic Institute and State University, VA, 1996.

[3] S.T. IJsselmuiden, *Optimal design of variable stiffness composite structures using lamination parameters*. PhD Thesis, Delft University of Technology, The Netherlands, 1996.

[4] H. Akhavan, P. Ribeiro, Natural modes of vibration of variable stiffness composite laminates. *Composite Structures*, **93**, 3040–3047, 2011.

[5] M.M. Abdalla, S. Setoodeh, Z. Gürdal, Design of variable stiffness composite panels for maximum fundamental frequency using lamination parameters. *Composite Structures*, **81**, 283–291, 2007.

[6] A.W. Blom, S. Setoodeh, J.M.A.M Hol, Z. Gürdal, Z, Design of variable-stiffness conical shells for maximum fundamental eigenfrequency. *Computers & Structures*, **86**, 870–878, 2008.

[7] S. Yazdani, P Ribeiro, Geometrically non-linear static analysis of unsymmetric composite plates with curvilinear fibres: p-version layerwise approach. *Composite Structures*, **118**, 74–85, 2014.

[8] S. Yazdani, P Ribeiro, J.D. Rodrigues, A p-version layerwise model for large deflection of composite plates with curvilinear fibres. *Composite Structures*, **108**, 181–190, 2014.

[9] B.F. Tatting, Z. Gürdal, *Automated finite element analysis of elastically-tailored plates*. NASA contractor report no NASA/CR-2003-212679, 2003.

[10] B.F. Tatting, Z. Gürdal, *Design and manufacture of elastically tailored tow placed plates*. NASA contractor report no NASA/CR-2002-211919, 2002.

[11] H. Akhavan, P. Ribeiro, Free geometrically nonlinear oscillations of perfect and imperfect laminates with curved fibres by the shooting method. *Nonlinear Dynamics*, **81**, 949–965, 2015.

[12] H. Akhavan, P. Ribeiro, Non-linear forced periodic oscillations of laminates with curved fibres by the shooting method. *International Journal of Non-Linear Mechanics*, **76**, 176–189, 2015.

[13] B.K. Stanford, C.V. Jutte, Comparison of curvilinear stiffeners and tow steered composites for aeroelastic tailoring of aircraft wings. *Computers & Structures*, **183**, 48–60, 2017.

[14] R.R. Fernandes, A.Y. Tamijani, Flutter analysis of laminated curvilinear-stiffened plates. *57th AIAA/ASCE/AHS/ASC Structures, Structural Dynamics, and Materials Conference*, San Diego, United States, January 4-8, 2016.

[15] B.K. Stanford, C.V. Jutte, W.K. Chauncey, Aeroelastic benefits of tow steering for composite plates. *Composite Structures*, **118**, 416–422, 2014.

[16] W. Han, M. Petyt, K.M. Hsiao, An investigation into geometrically nonlinear analysis of rectangular laminated plates using the hierarchical finite element method. *Finite Elements in Analysis and Design*, **18**, 273–288, 1994.

[17] P. Ribeiro, *Geometrical nonlinear vibration of beams and plates by the hierarchical finite element method*. PhD Thesis, University of Southampton, UK, 1998.

[18] E.H. Dowell, R. Clark, D. Cox, *A modern course in aeroelasticity*. Dordrecht: Kluwer academic publishers, 2004.

[19] J. Reddy, *Mechanics of laminated composite plates and shells: theory and analysis*. CRC Press, 2004.

[20] B. Vlasov, On the equations of bending of plates. *Dokla Ak Nauk Azerbeijanskoi-SSR*, **3**, 955–979, 1957.

[21] J. Rodrigues, P. Ribeiro, H. Akhavan, Experimental and finite element modal analysis of variable stiffness composite laminated plates. *Proceedings of the 11th Biennial International Conference on Vibration Problems (ICOVP-2013)*, Lisbon, Portugal, 2013.